Bull Volcanol (1996) 58:194–204

ORIGINAL PAPER

M. D. Higgins

Crystal size distributions and other quantitative textural measurements in lavas and tuff from Egmont volcano (Mt. Taranaki), New Zealand

Received: 25 October 1995 / Accepted: 19 April 1996

Abstract The size, shape and orientation of plagioclase crystals have been quantified in a tuff and series of andesite lavas from the active Egmont volcano (Mt. Taranaki), New Zealand. Linear crystal size distributions (CSDs) show that if the magma had several components, then only one provided the crystals. The slope of the CSD indicates that the earliest lavas measured had a residence time of ~50 years in the magma chamber for a growth rate of 10^{-11} cm/s. Subsequent lavas had slightly longer residence times (50–75 years), but the following series returned to 50-year residence times. The youngest magmas, from both Egmont summit and the parasitic Fantham's Peak, have the shortest residence times of ~30 years. Variations in residence time may reflect changes in the magma chamber shape or depth, or the temperature of the surrounding rocks. Crystal shapes and zonation suggest that crystallization occurred in a bottle-shape magma chamber, and not in a narrow conduit. If future eruptions use the same magma chamber as the most recent eruptions, then a delay of approximately 30 years can be expected between refilling and eruption.

Key words CSD · Residence time · Egmont volcano Mt. Taranaki · Crystal shape · Crystal orientation · Magma chamber

Introduction

The natural hazard potential of volcanoes is significant and many efforts are now being made to predict their behaviour, especially in this "Decade of Natural Hazard Reduction". One key aspect of the assessment of the hazards posed by a volcano is the timing of magma movements in the sub-surface. Seismic studies fill this role amply for current and recent eruptions, but we need to expand our knowledge to include older historic and pre-historic events. Crystal size distributions (CSD) can provide some information on timing of magma movements which have produced volcanic products on the surface, such as lavas and ashes (see review by Cashman 1990). A number of assumptions and numerical values of parameters are, of course, necessary; most important is the crystal growth rate. Recent advances in the determination of this parameter (Cashman 1993) have enabled magma residence times to be estimated from the size distribution of plagioclase crystals (Mangan 1990). The CSD technique is applied here to Mt. Taranaki (Egmont volcano), whose volcanic hazard potential is great (I. E. M. Smith, pers. commun.), but about which little has been published. It is shown herein how each of the different series of Holocene eruptions has a characteristic residence time and how these values can then be used to predict the future behaviour of the volcano.

Editorial responsibility: W. Hildreth

Michael D. Higgins
Sciences de la Terre, Université du Québec à Chicoutimi, Chicoutimi, G7H 2B1, Canada

The Taranaki volcanic field

Volcanism in the westernmost part of the North Island of New Zealand is related broadly to a major plate tectonic boundary which starts almost 3000 km to the north near Tonga (Cole 1990). In the north the boundary is a subduction zone which dips to the northwest. This zone continues southwards past the North Island, to the South Island, where it transforms into a strike-slip fault, the Alpine fault. The most important volcanic region related to this structure is the Taupo Volcanic zone, which is clearly distinct from the Taranaki volcanic field (Fig. 1). The Benioff zone lies at a depth of 180 km beneath the Taranaki volcanic field, but the reason for the existence of the volcanism in this area is not clear (Adams and Ware 1977).

The Taranaki volcanic field is composed of four volcanic edifices aligned approximately northwest–south-

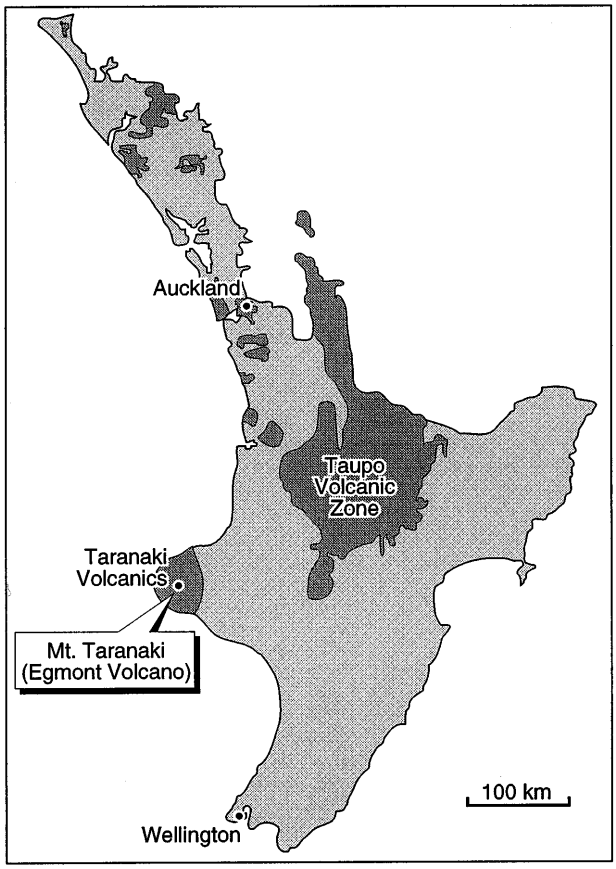

Fig. 1 Late Cenozoic volcanic rocks of the North Island of New Zealand. Mt. Taranaki (Egmont volcano) is the youngest part of the Taranaki volcanic field

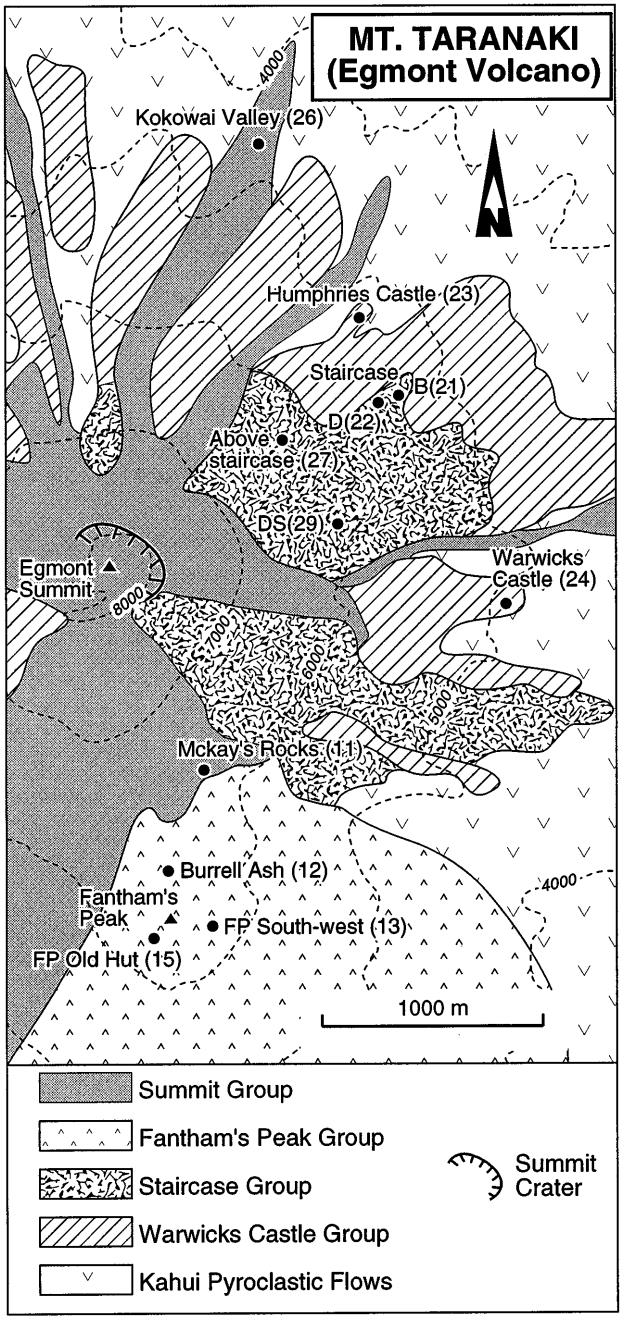

Fig. 2 The summit region of Mt. Taranaki (Egmont volcano). The parasitic cone of Fantham's Peak lies to the south of the summit. The names of the volcanic units sampled are followed by the sample number in *parentheses*. Contours are in feet above sea level. Geology from Stewart et al. (1996)

east, approximately parallel to the dip of the Benioff zone (Neall et al. 1986). Volcanism started in the northwest approximately two million years ago and has progressed to the southeast, culminating in Mt. Taranaki or Egmont, the only active volcano in this part of New Zealand (Neall et al. 1986). The mountain is usually known as Mt. Taranaki, but the volcano is called Egmont volcano.

Egmont volcano is 2520 m high and has the classical form of a stratovolcano, modified on the southern side by a subsidiary cone, known as Fantham's Peak (Fig. 2). The volcano started to form approximately 120000 years ago, but the main cone is only 10000 years old, and the volcano was last active in 1750 A.D. (Neall et al. 1986; Price et al. 1992). The steep sides of the volcano have shed tremendous quantities of material, forming wide surrounding plains now densely populated (Neall et al. 1986). Hence, the potential for volcanic hazards from debris flows is very high.

Egmont volcano

The chronology of lava flows of Egmont volcano is poorly known (Neall et al. 1986; Price et al. 1992), and attempts to refine it using secular magnetic field variations have only been partly successful (Fig. 3; Downey et al. 1994). The oldest flows exposed currently are a series of bluffs which almost encircle the mountain at an altitude of between 1500 and 2000 m, including Warwicks Castle and Humphries Castle (Fig. 2). These hornblende andesite flows are up to 100 m thick and have well-developed columnar jointing. Their lower

Time	Egmont Summit	Fantham's peak
1750 AD	Dome emplacement	
1655 AD	Burrell Ash	
	Summit Group	South-west flow
	Staircase Group	Old hut flow
1300 AD		
2800 BP		
	Warwick's Castle Group	
7000 BP		
120,000 BP	Birth of volcano	

Fig. 3 Approximate chronology of Egmont volcano (following Neall et al. 1986; Price et al. 1992; Downey et al. 1994)

edge is very abrupt, suggesting that they impounded against the front of the flow, now removed by erosion. Radiocarbon dates of plant remains underlying the flows indicate that the eruptions occurred approximately 7000 years ago (Fig. 3; Price et al. 1992).

Fantham's Peak (1950 m) is a large subsidiary vent on the southern slopes approximately 1.5 km south of the summit (Egmont summit; Fig. 2). It includes several vents and is dominated by basaltic andesites. It probably originated as early as 7000 years ago (Neall et al. 1986), and the last phase of activity was between 700 and 400 years ago (Downey et al. 1994).

Activity at the summit appears to have recommenced approximately 700 years ago (Downey et al. 1994). The earliest flows are the Staircase series, best exposed on the east side of the mountain (Figs. 2 and 3). These were partly covered by the Summit flows. The Burrell ash, which is now well exposed on the saddle between the summit and Fantham's Peak, erupted in 1655 A.D. The last magmatic event was the emplacement of a lava dome in the summit crater in 1750 A.D.

Petrology and geochemistry

Egmont volcano is dominated by hornblende andesites and basaltic andesites; minor basalts were not studied here (Neall et al. 1986). The most common crystalline phase in most samples is plagioclase (12–40%; Table 1; Neall et al. 1986). It occurs generally as euhedral, tabular crystals which vary widely in composition, with cores from An_{90} to An_{55} and rims as sodic as An_{30} (Neall et al. 1986; Stewart et al., unpublished). A moderate to strong preferred orientation of the long axes of the crystals indicates that they crystallized before eruption. Some crystals are completely clear, but most have one or more euhedral or rounded "dusty" zones of inclusions of other minerals, more sodic plagioclase or glass (Fig. 4). Such structures are seen in other volcanic rocks and have been termed "sieve" or "cellular" textures. Some of the clear zones have oscillatory zoning especially towards the edges of the crystals (Neall et al. 1986). In some crystals these zones cut inner structures indicating some resorption. Most crystals have different sequences and thicknesses of zones, indicating that each has an independent growth history. A few adjacent crystals are similar suggesting that they are linked out of the plane of the section as a glomerocryst.

Dusty zones are thought to be produced by destabilization of existing plagioclase following changes in the physicochemical environment of the crystal, such as mixing with more calcic (Tsuchiyama 1985) or hotter melts (Morrice and Gill 1986), or by increases in the

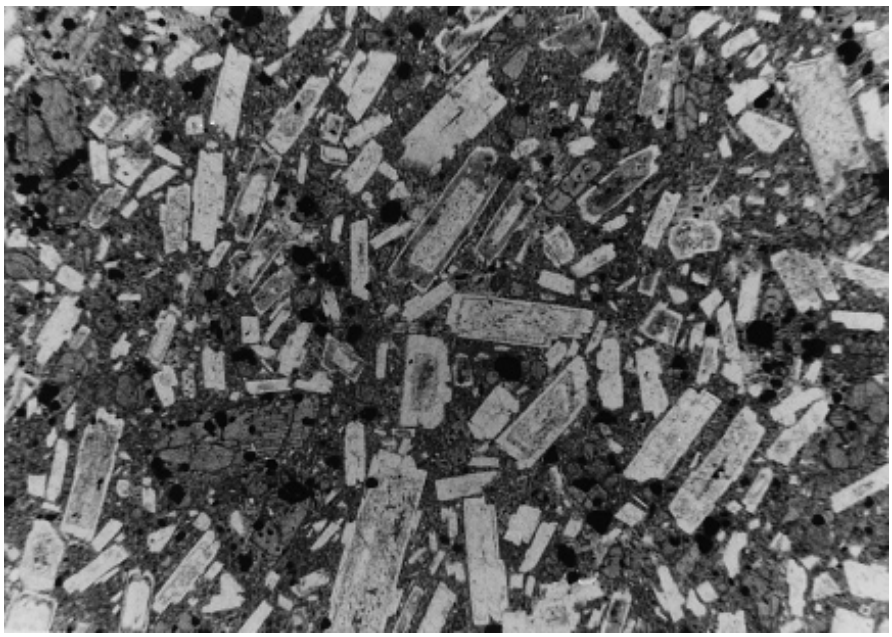

Fig. 4 Thin section photograph of andesite lava, Warwicks Castle flow (NZ24A). The most abundant phase is plagioclase, followed by clinopyroxene and titanomagnetite. Plane-polarized light. Field of view 6 mm

Table 1 Morphometrical and other parameters of the Taranaki samples. Areas measured varied from 48 to 64 mm^2

Volcanic units[a]	Volcanic group	No. of crystals counted	Crystallinity (%)[d]	Intercept Ln (mm^{-4})[e]	Slope (mm^{-1})[e]	Residence time (years)[f]	Preferred orientation[g]	Ratio orientation ellipse
Burrell ash (12)	1655 A.D. Ash	358	8.3	4.50 ± 0.22	−9.87 ± 0.29	32 ± 1	UOS	0.75
McKay's rocks (11)	Summit	495	24.6	3.90 ± 0.33	−5.60 ± 0.30	57 ± 3	−29	0.88
Kokowai, 10 cm (26A)[c]	Summit	255	14.4	3.97 ± 0.45	−7.18 ± 0.45	44 ± 3	+2	0.83
Kokowai, 100 cm (26B)[c]	Summit	345	20.7	3.86 ± 0.30	−6.29 ± 0.30	50 ± 2	−19	0.73
Kokowai, 100 cm (26B)[c], normal	Summit	289	11.4	4.12 ± 0.29	−6.90 ± 0.46	46 ± 3	+9	0.99
Kokowai, 250 cm (26C)[c]	Summit	305	20.1	3.92 ± 0.26	−6.68 ± 0.26	47 ± 2	+28	0.84
Above Staircase flow (27)	Staircase	130	15.0	2.06 ± 0.79	−4.85 ± 0.81	65 ± 13	−39	0.79
DS flow (29)	Staircase	263	17.9	3.23 ± 0.50	−6.03 ± 0.50	53 ± 5	UOS	0.88
Staircase flow B (22)	Staircase	147	16.1	1.91 ± 0.41	−4.25 ± 0.43	75 ± 8	+12	0.85
Staircase flow D (21)	Staircase	170	19.3	2.32 ± 0.48	−4.45 ± 0.47	71 ± 8	+37	0.76
FP[b] South–West flow (13A)	Fanthams Peak	610	9.8	4.97 ± 0.42	−8.90 ± 0.54	35 ± 2	ND	ND
FP Old Hut (15)	Fanthams Peak	611	14.9	6.17 ± 0.38	−12.24 ± 0.54	26 ± 1	−41	0.69
Warwicks Castle (24A)	Castle	553	30.2	4.82 ± 0.31	−6.90 ± 0.31	46 ± 2	+22	0.75
Humphries Castle, 10 cm (23C)[c]	Castle	401	28.5	4.16 ± 0.28	−6.22 ± 0.26	51 ± 2	−1	0.69
Humphries Castle, 70 cm (23B)[c]	Castle	630	26.6	4.67 ± 0.47	−6.99 ± 0.43	45 ± 3	−2	0.74
Humphries Castle, 200 cm (23A)[c]	Castle	267	17.8	2.95 ± 0.68	−5.42 ± 0.62	58 ± 8	+31	0.75

[a] All samples are lavas except the Burrell ash. Sample numbers are in parentheses. All samples were cut parallel to the flow direction in a vertical plane, except where indicated
[b] Fantham's Peak
[c] Height above the base of the flow
[d] The percentage by volume of plagioclase crystals longer than 0.125 mm, the lower cutoff for measurements
[e] Intercept and slope were calculated from a linear regression of the population density distributons, uncertainties are one-sigma errors
[f] Residence times were calculated using a crystallization rate of 10^{-11} cm/s
[g] Preferred orientation directions are positive for downstream inclination and negative for upstream inclination. In the case of the flow-normal section zero is horizontal. Two samples were not oriented in the field (UOS); hence, their preferred orientation direction has no meaning and was omitted
ND Not determined

total pressure or partial pressure of water (Morrice and Gill 1986), or by rapid reduction in pressure (Nelson and Montana 1992). Whatever the exact cause, the richness of variation among coexisting crystals suggests a dynamic environment of rapidly changing P–T–X conditions, such as might be expected in sub-volcanic reservoir which is being refilled with new magma and drained by eruptions.

Clinopyroxene is the next most abundant phase in most lavas, comprising 2–26% (Neall et al. 1986), but is occasionally sub-equal to the plagioclase. It is an augite or diopside-augite, commonly with oscillatory or sector zoning. Clinopyroxene crystals are similar in size to the plagioclase crystals. Titanomagnetite comprises 1–6% (Neall et al. 1986) and is commonly associated with clinopyroxene. Crystals are much smaller than the plagioclase or clinopyroxene.

Stewart et al. (1996) consider that the Egmont magmas crystallized plagioclase in the lower crust, rather than in a shallow magma chamber, as suggested herein. They consider that the core compositions of olivine crystals coexisting with the plagioclase indicate that the magmas were water-undersaturated (Morrice and Gill 1986), which contrasts with the hydrous conditions indicated by the amphibole. Hence, they conclude that the plagioclase crystallized from water-undersaturated melts in the lower crust. However, Price et al. (1992) consider that the Egmont volcano magmas have a mixed origin, in which case the arguments of Stewart et al. (1996) do not apply. The complex zonation of the

plagioclase crystals also suggests a dynamic environment more consistent with a shallow origin.

The geochemical signature of the Egmont volcano lavas and tuffs accords with their convergent plate margin tectonic setting (Price et al. 1992). Rare-earth diagrams do not show europium anomalies, indicating that significant quantities of plagioclase have neither been fractionated from the magma nor have accumulated in the magma (Price et al. 1992).

Morphometrical data

Methods

Samples were taken from unweathered parts of the lava flows and a pumice block from the Burrell ash. Most of the thin sections analysed in this study were oriented parallel to the flow direction, in a vertical plane. Swaths measuring approximately 4×15 mm were photographed and printed at a magnification of $\times 50$. The outlines of each crystal in this region were traced by hand from these photographs on a digitizing tablet connected to a computer. The length, width, area and perimeter of the crystal outline and the orientation of the trace of the albite-twin plane were calculated from the raw positional data using software written by this author. These data were then analysed using a specially written program (Inertia Tensor method, see later; Pierre-Yves Robin, unpublished) and a standard spreadsheet program.

Crystal size distributions

A theory of crystal size distributions (CSD) developed by Randolf and Larson (1971) and applied to magmatic systems by Marsh (1988) and Cashman and Marsh (1988) indicates that under certain circumstances the natural logarithm of the population density of crystals (i.e. the number of crystals within a size interval per unit volume divided by the width of the interval) varies linearly with the crystal length. For volcanic rocks the slope of this line can generally be equated with –1/(Growth rate * Typical crystal residence time) and the intercept corresponds to the nucleation density. The residence times of crystals, and hence magmas, in magma chambers are of great interest in the study of volcanoes. To extract residence times we must first determine the parameters of the CSD and then choose a suitable growth rate.

The population density is a volumetric measure, but crystal sizes and numbers are generally measured in two dimensions (e.g. in thin sections); hence, the raw data must be transformed. Therein lie two stereological problems: Firstly there are no exact transformations of two-dimensional (2D) population densities to three-dimensional (3D) values, except for spheres (Royet 1991). Most studies to date have used the simple transformation (Cashman 1990):

$$\text{Population density} = (\text{Number of crystals/Area})^{1.5}/\text{Length interval}$$

This equation has been used here to calculate the CSD diagrams, such as in Fig. 5, so that they can be readily compared with existing data.

Higgins (1994) has shown that the dominant length measured in 2D slices, such as thin sections, is not generally the true 3D length, but some other dimension. The Egmont volcano lavas have a strong linear fabric developed by flow of the crystal-rich magma. If all crys-

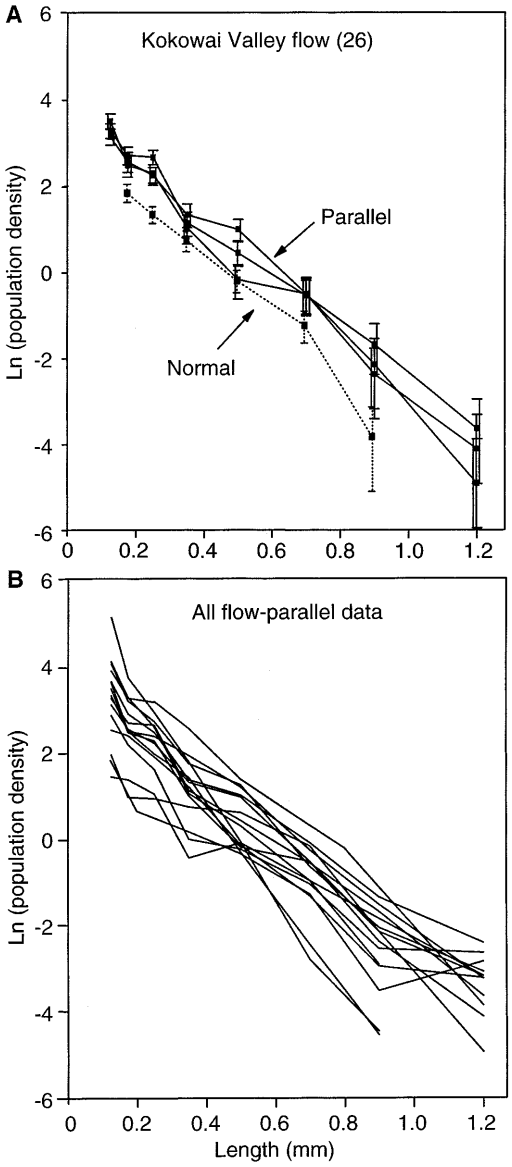

Fig. 5A, B Crystal size distribution (CSD) data. Note that both length scale and population density are in millimetres. **A** Four samples from near the base of the Kokowai Valley flow. *Error bars* are for one-sigma uncertainties. **B** All 15 flow-parallel samples from Egmont volcano, including those from the Kokowai Valley flow

tals are perfectly aligned, then in sections cut normal to this fabric the dominant length is the intermediate dimension, whereas in parallel-cut sections the observed length is the actual 3D length.

The contribution of small, off-centre intersections of large crystals to smaller crystal population density is dependent on crystal shape (Higgins 1994), a parameter which is rarely measured in CSD studies. Although the data presented herein could be corrected for this effect using the crystal shape (see later) and the curves of Higgins (1994), it would not then be possible to compare this data with that of existing studies, e.g. the growth rate studies of Cashman (1993; see below). Hence, it is assumed that this effect is relatively minor.

Choice of the correct growth rate is very important in the calculation of residence times: higher growth rates reduce the residences times proportionately. Cashman (1993) has shown that there is a good correlation between cooling rate, or its inverse crystallization time, and plagioclase growth rate in basaltic magmas. A cooling time of 3 years, perhaps typical of lava flows, would give a growth rate of 10^{-10} cm/s, whereas a cooling time of 300 years, perhaps typical of a sub-volcanic magma chamber, would yield a growth rate of 10^{-11} cm/s. Note that changing the cooling rate by a factor of 100 only changes the growth rate by a factor of 10. For comparison, growth rates of plagioclase in the Makaopuhi lava lake (Cashman and Marsh 1988) varied from 5×10^{-10} cm/s at a depth of 13.6 m (80% crystallized), to 1×10^{-10} cm/s at a depth of 16.6 m (20% crystallized). Cashman (1992) showed that growth rate scales with magma viscosity, but that there is less than an order of magnitude difference between basaltic and dacitic magmas. The viscosity difference between basalt and the andesites and basaltic andesites of Egmont volcano is much less; hence, the difference in growth rate must be quite small. Taking all these factors into account, a growth rate in the magma chamber of 10^{-11} cm/s has been selected. For those crystals which grew after the eruption, in the lava flows, a growth rate of 10^{-10} cm/s has been used.

Turning now to the data, the first question to be addressed must be the reproducibility of the data. Figure 5A shows the CSDs of three samples from the Kokowai Valley flow (Summit group), all cut parallel to the flow direction in a vertical orientation. The error bars are the square root of the number of crystals in each interval. The three CSDs are linear for crystal long axes greater than 0.125 mm, the smallest size which could be measured consistently (Fig. 5A). The samples are also co-linear, within analytical error, indicating that the data are reproducible for different samples with similar histories. A fourth section, cut normal to the flow direction, has a CSD below that of the parallel-cut sections (Fig. 5A). This is to be expected because the apparent length in flow-parallel sections is equal to true length, but only the intermediate dimension in flow-normal sections (Higgins 1994). If the lengths measured in this section are multiplied by 1.33, the ratio of the long to intermediate dimensions of the crystals at Egmont volcano (see later), then the flow-normal CSD is co-linear with the flow-parallel CSDs.

The CSDs of these three samples can also be used to determine whether there has been significant crystal growth after the eruption of the lava. The lowest sample was taken only 10 cm from the base of the flow, and hence represents the chilled margin. The other samples were taken at heights of 100 and 250 cm above the base of the flow, and hence must have taken much longer to crystallize. As mentioned previously, there is no significant difference between the CSDs of these three samples; hence, any crystal growth after eruption must have been restricted to crystals smaller than 0.125 mm or additions to existing crystals of less than this amount. At a growth rate of 10^{-10} cm/s, typical of cooling times on the surface (Cashman 1993), this length represents 3 years, which is greater than the crystallization times of most flows.

All the other samples from Egmont volcano are also linear for crystals longer than 0.125 cm (Fig. 5B). A linear regression of the CSDs gave the slope and intercept parameters, and their one-sigma errors are listed in Table 1. The slopes have been transformed into residence times using a growth rate of 10^{-11} cm/s (Fig. 6). The errors in the residence times are only those due to the regression of the CSD – uncertainties in the growth rate will systematically shift all the residences times to higher or lower values. There is strong correlation between residence time and Ln (nucleation density). This is to be expected because both parameters are controlled dominantly by cooling rate (e.g. Cashman 1993). The Staircase flows tend to have the longest residence times – up to 75 years (Fig. 6). The Fantham's Peak

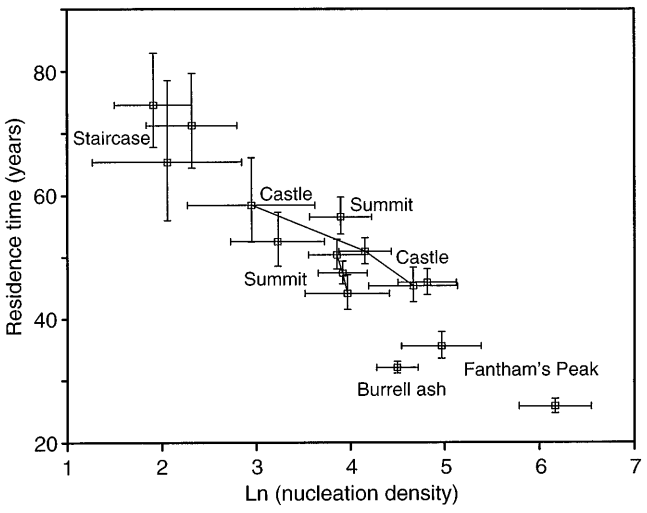

Fig. 6 Residence times and nucleation rates of samples from Egmont volcano. Residence times are based on a growth rate of 10^{-11} cm/s. *Error bars* are one-sigma uncertainties from the linear regression of the CSD curves in Fig. 4, and do not include systematic errors, such as those produced by an incorrect choice of the growth rate or by the 2D to 3D transformation

flows and the Burrell ash have the shortest residence times of 26–35 years. All other flows occupy the middle ground with residence times of 45–60 years.

Crystal shapes

The overall shape of particular crystalline compounds is determined by the physicochemical conditions of crystallization (Sunagawa 1987). Hence, determination of the crystal habit may reveal aspects of the crystallization environment. The crystal shape may be estimated from the parameters of the 2D width/length ratio distributions (Higgins 1994).

Width/length ratio distributions for all 15 of the flow-parallel samples are all very similar (Fig. 7); hence, the data were amalgamated to improve the precision. A plot of log (area) vs log (perimeter) of the amalgamated data was used to determine if there are significant variations in crystal shape for different sizes (Fig. 8). A regression of the data gave a slope of one half, indicating that crystal shape does not vary with size.

Returning to the width/length distributions, the mode of the flow-parallel data is 0.33, which is equal to the ratio short/long for a linear fabric (Higgins 1994). The mode of the flow-normal section is 0.5, equal to the ratio short/intermediate (Fig. 7). These data indicate an overall aspect ratio of 1:2:3, i.e. slightly elongated tablets (Higgins 1994). Examination of thin sections shows that the crystals are flattened parallel to the (010) face, or *b*–axis, but the elongation in the plane of the tablet is not clear. Prismatic crystals, such as those from Kameni volcano (Higgins 1996), are elongated along the *a*–axis; hence, the probable ordering of axial dimensions is a > c > b, that is, a = L, b = S and c = I.

Crystal orientations

The Inertia Tensor method was used to determine the direction of the preferred orientation and the coherence of crystal orientations in the plane of the section (Pierre-Yves Robin, unpublished). These data were calculated from the digitized crystal outlines (F. Fueten, pers. commun.). This technique has the advantage that the contribution of each crystal to the total orientation ellipse is weighted for its elongation. The coherence of the crystal orientations was quantified by the ratio of the orientation ellipse axes: a sample with well-aligned crystals has an elongated orientation ellipse, and hence low values of the ratio of orientation ellipse axes (minor axis/major axis), whereas a sample without preferred orientation directions in the plane of interest will have circular orientation ellipse and hence an axial ratio of one.

In all flow-parallel samples there was a preferred orientation of the crystals within 41° of the flow direction, with approximately equal numbers of samples inclined upstream and downstream (Fig. 9; Table 1). Crystal orientation coherence was variable, with ratios of orientation ellipse axes from 0.69 to 0.88. There was no preferred orientation in flow-normal section, confirming the linear fabric expected for crystal-rich lavas which have flowed.

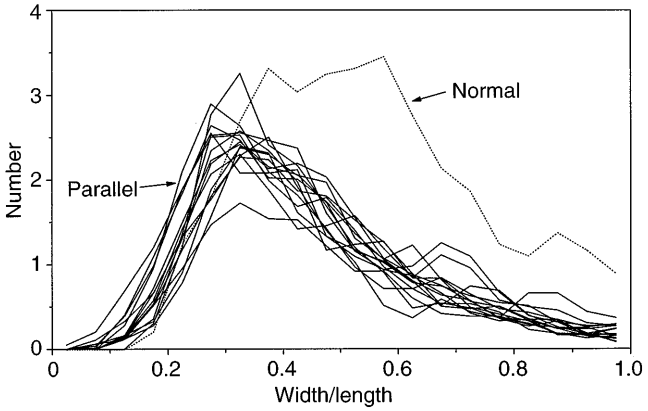

Fig. 7 Width/length distributions for all the samples from Egmont volcano. The *vertical axis* is the number of crystals in each interval divided by the total number of crystals and the class width

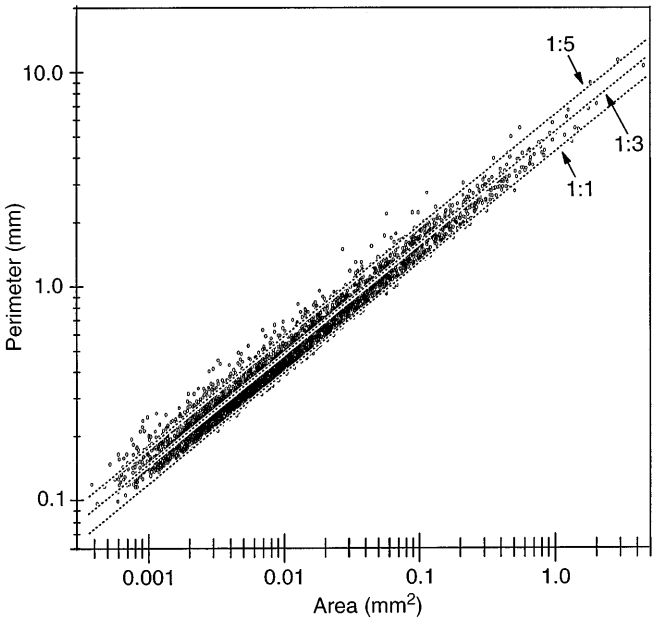

Fig. 8 Area vs perimeter of plagioclase crystals from all samples

Discussion

Residence times

The linear CSDs of the Egmont volcano lavas and tuff, for plagioclase crystal lengths greater than 0.125 mm, indicates that one crystal population dominates the

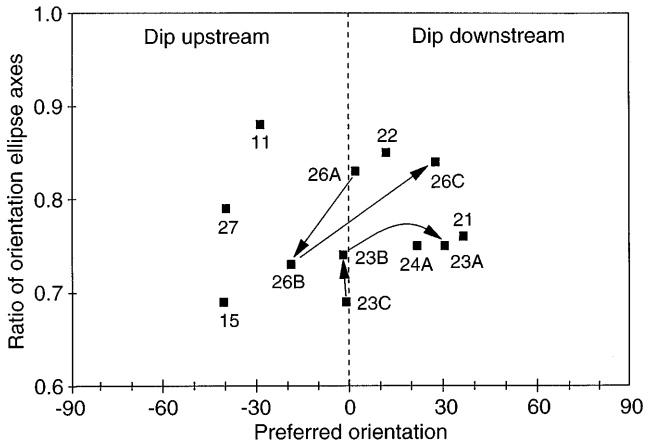

Fig. 9 Plagioclase crystal orientation data, as derived by the Inertia Tensor method (Robin, unpublished). The *vertical axis* is the ratio minor axis/major axis of the orientation ellipse. A value of one indicates no preferred orientation. *Arrows* indicate ascending order of samples in the two lava-flow sections

magmas and that it formed under constant conditions of crystallization, such as cooling rate. Of course, some crystallization occurred following eruption, but it has already been shown that this was restricted to crystals smaller than 0.125 mm. These linear CSDs contrast with the curved CSDs found in lavas from some other volcanoes which have been interpreted to reflect variable cooling rates (Armienti et al. 1994) or magma mixing (Higgins 1996).

Although the CSDs of the Egmont volcano samples are simple, the internal structures of the plagioclase crystals (dusty zones, oscillatory zonation) are complex. Price et al. (1992) suggested that this is related to magma mixing, but find no geochemical evidence for this process. The simple CSDs do not support this idea either, unless one magma was free of crystals. It is also possible that the complex internal structures of the plagioclase may have been produced by circulation of crystal-bearing magma within a chamber. For example, the magma chamber beneath Mount St. Helens volcano is bottle-shaped, with the main section extending from 7 to 14 km in depth (Pallister et al. 1992). Magmatic convection in such a chamber involves major changes in pressure, which can produce the dusty zones observed in the plagioclase crystals (Nelson and Montana 1992). Such a model could also account for the contrasting history of most crystals, as recorded by their internal sequence of zones.

The magma chambers which produced the Kokowai Valley, Warwicks Castle and Humphries Castle flows appear to have been similar, with residence times of ~50 years (Table 1). The residence time of the magma chamber which produced the Staircase flows was slightly greater, 50–75 years. After that the residence times returned to ~50 years for the Summit flows and finally to ~30 years for the Burrell ash and Fantham's Peak flows. The changes in residence time, if significant, may represent changes in the shape and/or depth of the magma chamber or the temperature of the surrounding rock.

The magma residence times of the Egmont volcano lavas and tuff may be used to predict the timing of future eruptions after a refilling event has been detected, i.e. by seismic techniques. If the eruption was similar to the last explosive eruption of Egmont summit, which produced the Burrell ash, or the latest eruptions of Fantham's Peak, then a delay of approximately 25–35 years could be expected between the refilling event and the eruption. If the eruption resembled more those that produced the Staircase lava sequence, then a delay of 60–80 years could be expected.

The residence times of the Egmont volcano magmas may be compared with those of other volcanoes (Table 2). Megacrysts in mixed-magma porphyritic dacite lavas from the Kameni volcano, Thera, Greece, gave similar residence times of 24–96 years (Higgins 1996). Microlites from these same rocks gave residence times of 6–13 years. Mangan (1990) and Resmini and Marsh (1995) established residence times for basaltic magmas which are shorter: 7–15 years at Kilauea, Hawaii, and

Table 2 Residence times of volcanic rocks from CSD measurements for two different growth rates. Residence times in italics are not those quoted in the paper but instead are recalculated for a different growth rate

Volcanic unit	Mineral	Residence times (years)		Reference
		10^{-10} cm/s	10^{-11} cm/s	
Egmont volcano, New Zealand	Plagioclase	*3–7*	26–75	This paper
Kameni volcano, Greece	Plagioclase megacrysts	*2–10*	24–96	Higgins (1996)
Kameni volcano, Greece	Plagioclase microlites	*0.6–1.3*	6–13	Higgins (1996)
Kilauea, Hawaii	Olivine	7–15	*70–150*	Mangan (1990)
Dome Mountain, Nevada	Plagioclase	1.5–4	*15–40*	Resmini and Marsh (1995)

1.5–4 years at Dome Mountain, Nevada. However, they used a growth rate for olivine and plagioclase ten times greater than that used herein. If the same growth rate is used, then the residence times bracket those of Egmont volcano. It will be difficult to compare these values exactly until we have a better understanding of growth rate variations. However, the two growth rates used in Table 2 span the range of most probable values.

Crystal shapes

Very little data is available on the shapes of plagioclase crystals in igneous rocks: A compilation of available data is shown in Fig. 10. Similarly, there has been little theoretical work on the equilibrium shapes of plagioclase. The closest material thus far discussed is analbite, the high-temperature polymorph of albite, which is elongated along the *c*–axis and hence has a c/a ratio greater than one and does not plot on this diagram (Fig. 10; Woensdregt 1992). The Egmont volcano plagioclase crystals are slightly more equant than the megacrysts from Kameni volcano (Higgins 1996). Plutonic plagioclase appears to fall into a slightly different field, with more prismatic crystals (Higgins 1994). Only partial shape data is available for plagioclase from Mt. Etna phonolites, but the short/intermediate ratios appear to be similar to that of the Egmont volcano rocks, whereas plagioclase from the Mauna Loa basalts is more tabular.

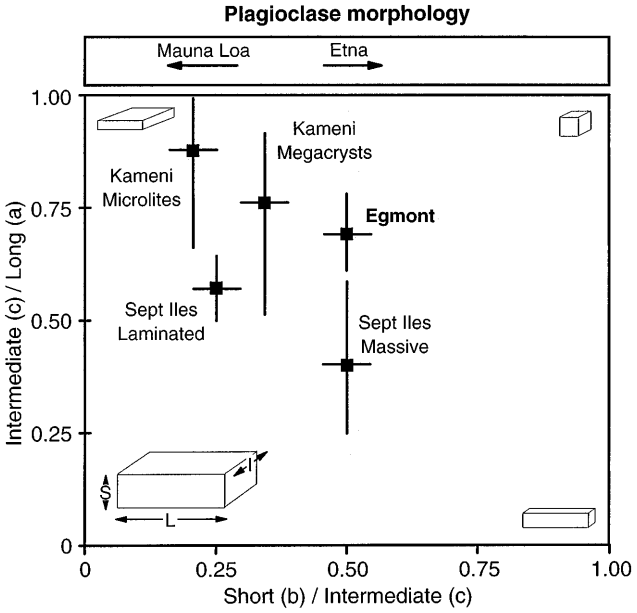

Fig. 10 Plagioclase crystal morphology in terms of the three major dimensions and crystallographic axes. Schematic crystal shapes are indicated in the *four corners*: clockwise form the top right they are cube, prism, flattened prism and tablet. Shapes of plagioclase crystals in other rocks are included: laminated and massive anorthosite in the Sept Iles complex (Higgins 1994); microlites and megacrysts from porphyritic dacite lavas of Kameni volcano, Greece (Higgins 1996). The *upper part* of the figure contains incomplete shape data lacking the intermediate/long parameter. Etna data from Armienti et al. (1994) and Mauna Loa data from Cashman (1990). *Arrows* indicate the range in values from smaller to larger crystals

Kouchi et al. (1986) has shown that mechanical movement of magma during crystallization is an important control on crystal shape, producing less equant crystals. Such shearing movements must be sufficiently intense to remove parts of the depleted zones around the growing crystal, and probably only occur close to the margins of magma chambers, in narrow conduits, or in lava flows. The relatively equant shape of the Egmont volcano plagioclase suggests that they grew in an environment without strong shearing. This excludes crystallization during flow in a conduit, but not in a magma chamber where convective magma movements involve less shear.

Crystal orientations

Orientation of the plagioclase crystals in the Egmont volcano lavas was dominantly produced by mechanical flow during eruption, although limited epitaxial nucleation in the magma chamber has produced some stacks of parallel crystals. Hence, the crystal orientation has a totally different origin from the CSDs and crystal shapes previously discussed.

The lack of exact information on the stratigraphic position of most of the samples makes the orientation data difficult to interpret, except to say that there does not appear to be any correlation between the direction of the preferred orientation and its coherence (ratio of orientation ellipse axes; Fig. 9).

Vertical sections of three samples taken from two different flows give much more information (Figs. 9 and 11). In the Kokowai Valley flow a sample near the base (26A) has a foliation almost parallel to the sole of the flow. The preferred orientation in a sample taken at a height of 100 cm (26B) tilts at 20° upstream, and a third, at 250 cm (26C), inclines downstream at 30°. The Humphries Castle flow has a similar structure: The preferred orientation of two samples taken at 10 and 70 cm (23C, 23B) are both parallel to the sole of the flow, whereas a third, taken at a height of 200 cm (23A), inclines downstream at 30°.

In both cases the preferred orientations direction showed a consistent pattern: Near the base the crystals are oriented parallel to the sole of the flow, but above a height of 1–2 m the preferred orientation dips at approximately 30° in a downstream direction (Fig. 11). The significance of the intermediate sample from the Kokowai Valley flow which dips upstream at approximately 20° is not clear. The coherence of orientation data does not appear to correlate with sample position. These orientations indicate that the flow advanced with a rolling motion: crystals were aligned during flow further upstream and then rolled over the stagnant zone close to the base of the flow.

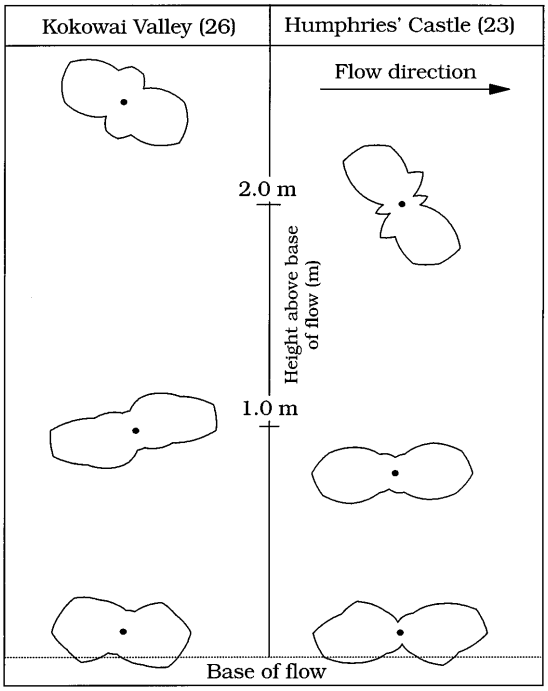

Fig. 11 Crystal orientations in flow-parallel samples from the base of two lava flows. Distance from the origin of each point on the surface is proportional to the number of crystals with that orientation

Conclusions

The following conclusions were reached as a result of this work:

1. The linear CSDs of the lava and tuff samples indicate that the magmas are dominated by one component. If magma mixing occurred, then one component must have been free of crystals or volumetrically unimportant. The complex internal zones of the plagioclase crystals may have been produced by crystallization during convective flow in a bottle-shaped magma chamber similar to that proposed to underlie Mount St. Helens volcano (Pallister et al. 1992).
2. Residence times of magmas in the sub-volcanic chamber vary from 26 to 75 years, when calculated using a growth rate of 10^{-11} cm/s. The residence times of the early magmas were around 50 years. The next series of magmas had slightly longer residence times of 50–75 years, but later returned to ~50 years. The most recent volcanic products from both the Egmont summit and Fantham's Peak have the shortest residence times – approximately 30 years. Residence time variations are due probably to changes in the shape and/or depth of the magma chamber and the temperature of the surrounding rocks.
3. Future eruptions, if they follow the model of the most recent eruptions, can be expected to have a residence time of approximately 30 years. If the refilling event can be detected, e.g. by seismic techniques, the approximate timing of the eruption may be predicted.
4. The tabular shape of the plagioclase crystals in the Egmont volcano lavas suggests that they grew in an environment without major shearing. This is consistent with growth in a gently convecting magma chamber, and not in a narrow conduit.
5. The orientation of plagioclase crystals in two sections at the base of thick lava flows are consistent: Flow is clearly parallel to the sole of the flow near the base, but is inclined downhill higher up. This suggests that the lava flow rolled downwards on the existing stagnant base.

Acknowledgements The thin sections were digitized patiently by Dominic Babin, Stefan Poirier and Josée Désgagné. Ian Smith, Richard Price and Bill Downey helped in the field. I thank Bob Stewart, Margaret Mangan and Akihiko Tomiya for their comments on the manuscript. Pierre Robin and Frank Fueton helped with the Inertia Tensor method. This project was financed by a grant from the Natural Science and Engineering Research Council of Canada.

References

Adams RD, Ware DE (1977) Structural earthquakes beneath New Zealand: locations determined with a laterally inhomogeneous velocity model. New Zealand J Geol Geophys 20:59–83

Armienti P, Pareschi MT, Innocenti F, Pompilio M (1994) Effects of magma storage and ascent on the kinetics of crystal growth. Contrib Mineral Petrol 115:402–414

Cashman KV (1992) Groundmass crystallisation of Mount St Helens dacite 1980–1986: a tool for interpreting shallow magmatic processes. Contrib Mineral Petrol 109:431–449

Cashman KV (1990) Textural constraints on the kinetics of crystallisation of igneous rocks In: Nicholls J, Russell JK (eds) Modern methods of igneous petrology: understanding magmatic processes. Rev Mineral 24:259–314

Cashman KV (1993) Relationship between plagioclase crystallisation and cooling rate in basaltic melts. Contrib Mineral Petrol 113:126–142

Cashman KV, Marsh BD (1988) Crystal size distribution (CSD) in rocks and the kinetics and dynamics of crystallisation. II. Makaopuhi lava lake. Contrib Mineral Petrol 99:292–305

Cole JW (1990) Structural control and origin of volcanism in the Taupo Volcanic zone, New Zealand. Bull Volcanol 52:445–459

Downey WS, Kellett RJ, Smith IEM, Price RC, Stewart RB (1994) New palaeomagnetic evidence for the recent eruptive activity of Mt Taranaki, New Zealand. J Volcanol Geotherm Res 60:15–28

Higgins MD (1994) Determination of crystal morphology and size from bulk measurements on thin sections: numerical modelling. Am Mineral 79:113–119

Higgins MD (1996) Magma dynamics beneath Kameni volcano, Greece, as revealed by crystal size and shape measurements. J Volcanol Geotherm Res 70:37–48

Kouchi A, Tsuchiyama A, Sunagawa I (1986) Effects of stirring on crystallization of basalt: texture and element partitioning. Contrib Mineral Petrol 93:429–438

Mangan MT (1990) Crystal size distribution and the determination of magma storage times: The 1959 eruption of Kiluea volcano, Hawaii. J Volcanol Geotherm Res 44:295–302

Marsh BD (1988) Crystal size distribution (CSD) in rocks and the kinetics and dynamics of crystallization. I. Theory. Contrib Mineral Petrol 99:277–291

Morrice MG, Gill JB (1986) Spatial patterns in the mineralogy of island arc magma series: Sangihe Arc, Indonesia. J Volcanol Geotherm Res 29:311–353

Neall VE, Stewart RB, Smith IEM (1986) History and petrology of the Taranaki volcanoes In: Smith IEM (ed) Late Cenozoic volcanism in New Zealand. R Soc N Z Bull 23:251–263

Nelson ST, Montana A (1992) Sieve textured plagioclase produced in volcanic rocks by rapid decompression. Am Mineral 77:1242–1249

Pallister JS, Hoblitt RP, Crandell DR, Mullineaux DR (1992) Mount St Helens a decade after the 1980 eruptions: magmatic models, chemical cycles, and a revised hazards assessment Bull Volcanol 54:126–146

Price RC, McCulloch MT, Smith IEM, Stewart RB (1992) Pb–Nd–Sr isotopic compositions and trace element characteristics of young volcanic rocks from Egmont volcano and comparisons with basalts and andesites from the Taupo volcanic zone, New Zealand. Geochim Cosmochim Acta 56:941–953

Randolf AD, Larson MA (1971) Theory of particulate processes. Academic Press, New York

Resmini RG, Marsh BD (1995) Steady-state volcanism, paleoeffusion rates and magma system volume inferred from plagioclase crystal size distributions in mafic lavas: Dome Mountain, Nevada. J Volcanol Geotherm Res 68:273–296.

Royet J-P (1991) Stereology: a method for analysing images. Progr Neurobiol 37:433–474

Stewart RB, Price RC, Smith IEM (1996) Evolution of High-K Arc Magma, Egmont Volcano, Taranaki, New Zealand: Evidence From Mineral Chemistry. J Volcanol Geotherm Res (in press)

Sunagawa I (1987) Morphology of crystals. Reidel, Dordrecht, The Netherlands

Tsuchiyama A (1985) Dissolution kinetics of plagioclase in the melt of the system Di–Ab–An and the origin of dusty plagioclase in andesites. Contrib Mineral Petrol 89:1–16

Woensdregt CF (1992) Structural morphology of analbite: the influence of the substitution of K by Na on the crystal morphology of alkali feldspars. Z Kristallogr 201:1–7